Materials Chemistry and Physics 111 (2008) 213–217

Contents lists available at ScienceDirect

Materials Chemistry and Physics

journal homepage: www.elsevier.com/locate/matchemphys

Electrochemical studies on cathode blends of $LiMn_2O_4$ and $Li[Li_{1/15}Ni_{1/5}Co_{2/5}Mn_{1/3}O_2]$

Soo Kyung Jeong[a], Jae Sun Shin[a], Kee Suk Nahm[a,*], T. Prem Kumar[b], A. Manuel Stephan[b]

[a] School of Chemical Engineering and Technology, Specialised Graduate School of Hydrogen and Fuel Cell Engineering, Chonbuk National University, Chonju 561-756, South Korea
[b] Electrochemical Power Systems Division, Central Electrochemical Research Institute, Karaikudi 630006, India

ARTICLE INFO

Article history:
Received 7 September 2007
Received in revised form 6 March 2008
Accepted 20 March 2008

Keywords:
Blend cathode material
XRD
Discharge capacity
Cyclic voltammetry

ABSTRACT

Composite cathodes were prepared by blending $LiMn_2O_4$ spinel and $Li[Li_{1/15}Ni_{1/5}Co_{2/5}Mn_{1/3}O_2]$ layer by simple mixing/ball milling followed by calcination at 800 °C. The prepared blend materials were subjected to XRD and charge–discharge studies. The cycling results revealed that the discharge capacity and cycleability of $LiMn_2O_4$ can be considerably increased upon blending the material with layered $Li[Li_{1/15}Ni_{1/5}Co_{2/5}Mn_{1/3}O_2]$.

1. Introduction

Layered manganese oxide cathodes are recognized as attractive cathode materials for lithium batteries because of its appealing properties like high theoretical capacity, low cost, non-toxicity, high voltage and capacity and higher lithium ion diffusion through van der Waal's gaps [1,2]. The layered $LiCoO_2$, although offers low irreversible capacity loss and good cycling profile, its high cost and toxicity still remain a problem area [3–5]. Similarly $LiNiO_2$ has its own limitations [6,7].

On the other hand the spinel compound $LiMn_2O_4$ and its derivatives have been identified as potential candidate materials because of its three dimensional Li^+-diffusion, low cost, abundance and non-toxicity which can store 110 mAh g^{-1} of charge on cycling [8–10]. However, it changes from spinel structure to layer upon prolonged cycling. Attempts have also been made to circumvent this problem more than a decade. Recently attempts have been made to exploit the advantages of both materials by blending both layered and spinel oxide materials.

Layered transition metal oxides, $LiMO_2$ (M = Co, Ni, Mn), and isotypic with α-$NaFeO_2$ are recognized as attractive cathode materials for lithium batteries. $LiCoO_2$ and $LiNiO_2$, with theoretical capacities of 274 mAg g^{-1}, are among the most investigated cathode materials. Although $LiCoO_2$ presents advantages such as east of preparation and a structure robust enough to withstand extended cycling in the limited range ($0.0 < x < 0.5$ in Li_xCoO_2) its high cost and toxicity prevent its extensive use, especially for consumer applications. On the other hand, nickel is not only cheap but also environmentally benign. However, stoichiometric $LiNiO_2$ is difficult to prepare [11,12]. A late entrant into this series is $LiMnO_2$. This compound presents appealing properties such as high capacity (290 mAh g^{-1}), low cost, non-toxicity, high voltage and high rate of lithium diffusion through van der Waal's gaps [13]. However, the structure of this material is unstable at high temperatures and is relatively difficult to synthesis. Therefore the attention gradually shifted to the exploitation of layered compounds with Co, Ni and Mn [14,15].

However, only a very few reports are available on blending of cathode materials. Ma et al. [16] reported the electrochemical properties of $LiMn_2O_4$ and $LiNi_{0.8}Co_{0.2}O_2$ materials in which the authors observed at least three-step electrochemical lithium extraction/insertion reaction during cycling. In a similar study Numata et al. [17] emphasized the importance of blending $LiNi_{0.8}Co_{0.2}O_2$ with $Li_{1+x}Mn_{2-x}O_4$. In an attempt to exploit advantages of both $LiNi_{0.8}Co_{0.15}Al_{0.05}$ layer and $Li_{1.1}Mn_{1.9}O_4$ spinel, Myung et al. [18] examined the cycling behavior of blend cathode materials. Surprisingly the authors have observed even though the positive electrode is composed of 50 wt.% of spinel oxide, over 96% of its initial capacity was maintained during 300 cycles.

Our recent study [2] and other reports [19] clearly reveal that the electrochemical behavior of layered compounds is strongly influenced by the method of preparation, as well as the heat treatments. The crystallinity, phase purity, particle morphology, grain size, sur-

* Corresponding author. Fax: +82 63 270 2306.
E-mail address: nahmks@chonbuk.ac.kr (K.S. Nahm).

0254-0584/$ – see front matter © 2008 Elsevier B.V. All rights reserved.
doi:10.1016/j.matchemphys.2008.03.032

face area, and cation distribution in the spinel structure, all of which can impact on the electrochemical performance of the compound are strongly determined by the synthesis procedure [2,19].

Many reports are available on the synthesis of layered manganese oxides and substituted oxide materials using hydroxide co-precipitation method [20,21], carbonate co-precipitation method [22] and combustion method [23], hydrothermal synthesis [24] and solid-state reaction method [8,25]. The materials prepared by solid-state method are not of uniform size and poor in stoichiometry. On the other hand the materials prepared by sol–gel method have several advantages such as good stoichiometry and uniform particle size. Our recent studies [2,26] reveal that the electrochemical and structural properties of lithium ion doped in transition metal layers are different from that of undoped in the transition metal layers. Furthermore, this type of materials can be synthesized with typical rhombohedral structure and can show monotonous charge–discharge behavior. So far to the best of our knowledge no attempt has been made on blending the $LiMn_2O_4$ with the layered manganese oxide material in which lithium is doped in the transition metal layer sites. Hence in the present study both spinel $LiMn_2O_4$ and layer $Li[Li_{1/15}Ni_{1/5}Co_{2/5}Mn_{1/3}O_2]$ are blended and their electrochemical studies have been analyzed.

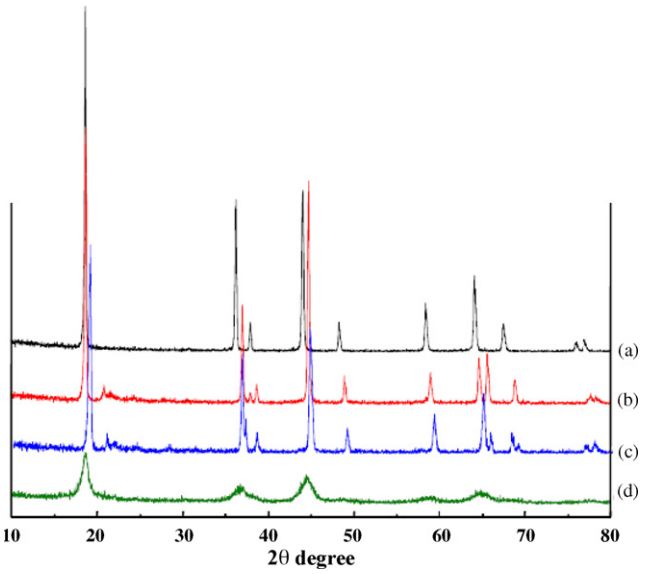

Fig. 1. Powder X-ray diffractograms of (a) sample S1, (b) sample S2, (c) sample S3 and (d) sample S4.

2. Experimental procedure

The $LiMn_2O_4$ and $Li[Li_{1/15}Ni_{1/5}Co_{2/5}Mn_{1/3}]O_2$ were prepared by a sol–gel method using glycolic acid as a chelating agent. Stoichiometric amounts of $CH_3COOLi{\cdot}2H_2O$ (Kanto, Japan), $(CH_3COO)_2Ni{\cdot}4H_2O$ (Aldrich, USA), $(CH_3COO)_2Co{\cdot}4H_2O$ (Aldrich, USA), and $(CH_3COO)_2Mn{\cdot}4H_2O$ (Acros, Belgium) were dissolved in DI water. The dissolved solutions were added drop by drop into the continuously agitated aqueous solution of glycolic acid. The metal:chelating agent was fixed to be 1:1. Initially, the pH of the solution was around 2. The pH of the solution was adjusted in the range of 5.5–7 by using ammonium hydroxide. Then the prepared solution was evaporated at 70–80 °C. The resulting precursors were heated with a heating rate of 1 °C min^{-1} and decomposed at 450 °C for 10 h in air. Thus, the decomposed powders were calcined for 10 h at 950 °C and quenched to room temperature. The powder X-ray diffraction (XRD, D/Max 2500, Rigaku) measurement using Cu Kα radiation was employed to characterize the crystalline phase of the synthesized material.

The electrochemical characterization was carried out using 2032-type coin cell (Hohsen). For the fabrication of cathode electrode, 20 mg of prepared $Li[Li_{0.07}Ni_{0.1}Co_{0.6}Mn_{0.23}]O_2$ materials were mixed with 12 mg of conductive binder (8 mg of tefronized acetylene black (TAB) and 4 mg of graphite). The mixture was pressed on 20 mm^2 Al mesh used as the current collector and dried at 100 °C for 10 h in a vacuum oven. The cells composed of cathode and the lithium foil (Cyprus Foote Mineral) anode, separated by porous polypropylene film separator (Celgard 3401) with an electrolyte of 1 M $LiPF_6$–ethylene carbonate (EC)/dimethyl carbonate (DMC) with a 1:2 volume ratio (Merck) were assembled in an argon-filled dry box and tested at room temperature. Thus prepared cells were charged and discharged at a current density of 0.4 mA cm^{-2} within the voltage ranges between the 2.5 and 4.5 V.

3. Results and discussions

3.1. XRD analysis

Fig. 1(a–d) shows the XRD patterns of $LiMn_2O_4$, $Li[Li_{1/15}Ni_{1/5}Co_{2/5}Mn_{1/3}]O_2$ and the blend of $LiMn_2O_4 + Li[Li_{1/15}Ni_{1/5}Co_{2/5}Mn_{1/3}]O_2$ by simple mixing and $LiMn_2O_4 + Li[Li_{1/15}Ni_{1/5}Co_{2/5}Mn_{1/3}]O_2$ calcined after ball milling, respectively. All the peaks are indexable in the *Fd*3*m* space group with a cubic lattice and the widths of the peaks are narrow, indicating the crystallinity of the material. It can be seen from Fig. 1(b) that all diffraction peaks are indexed to a hexagonal α-$NaFeO_2$ structure except the peaks between 21° and 25°. The broad XRD peaks between 21° and 25° are superstructure peak, resulting from superlattice ordering of Li, Ni, Mn atoms on the transition-metal layers. The main peaks (0 0 3) and (1 0 4) appear at $2\theta = 18°$ and 45°, respectively.

According to Morales et al. [27] the (0 0 3) peak occurs from the diffraction of the layered rock-salt structure (*R*3*m*), whereas the (1 0 4) peak occurs from both the diffraction of layered and cubic rock-salt structure. Also of importance the clear splitting of the lines assigned to Miller indices (0 0 6), (1 0 2) and (1 0 8), (1 1 0) is a characteristic feature of typical layered structure. Interestingly, it can be seen from Fig. 1(c) that the XRD patterns reflect the characteristic peaks of both spinel and layered structures. On the other hand, we observe a decrease in intensity as well as broadening of the XRD peaks for the sample ball milled after blending and calcinations (Fig. 1(c)). It has been shown that these nanocrystalline grains and the strain, that develops at grain boundaries, give rise to XRD peak broadening. The formation of nanograins through ball milling may be due to two processes: (i) the particles are broken into nano particles, which may subsequently adhere back together and, (ii) during the ball milling process because of hard agglomerates, many nanograins could have been generated within larger crystals due to the action of defects [9]. These results are in accordance with Manuel et al. [8] where the authors have reported the cycling behavior of ballmilled $LiMn_2O_4$.

3.2. Cyclic voltammetry

Typical plots of d*Q*/d*V* curves vs. voltage in the range of 2.5–4.5 V cyclic voltammograms for the samples A, B, C and D are shown in Fig. 2(a–d) respectively. The anodic and cathodic peak, respectively, shows the reversible oxidation and reduction of lithium extraction and reduction. It is obvious from Fig. 2(a) that the lithium extraction and insertion take place in three stages. The peak at lower potentials is assigned to the $Mn^{3+/4+}$ couple [28,29]. The second peak at 4.05 V is attributed to the removal of lithium ion from the tetrahydral sites from which Li–Li interactions occur. The third peak which is observed at 4.18 V is due to the removal of lithium ions from the other tetrahydral sites in which lithium ions do not have Li–Li interactions. The area of the oxidation and reduction peaks seem to be equal and in each stage lithium ions occupy half of the totally available crystallographic sites which is a characteristic feature of $LiMn_2O_4$ with high degree of crystallinity [30,31] On the other hand from Fig. 2(b) (sample S2) during the

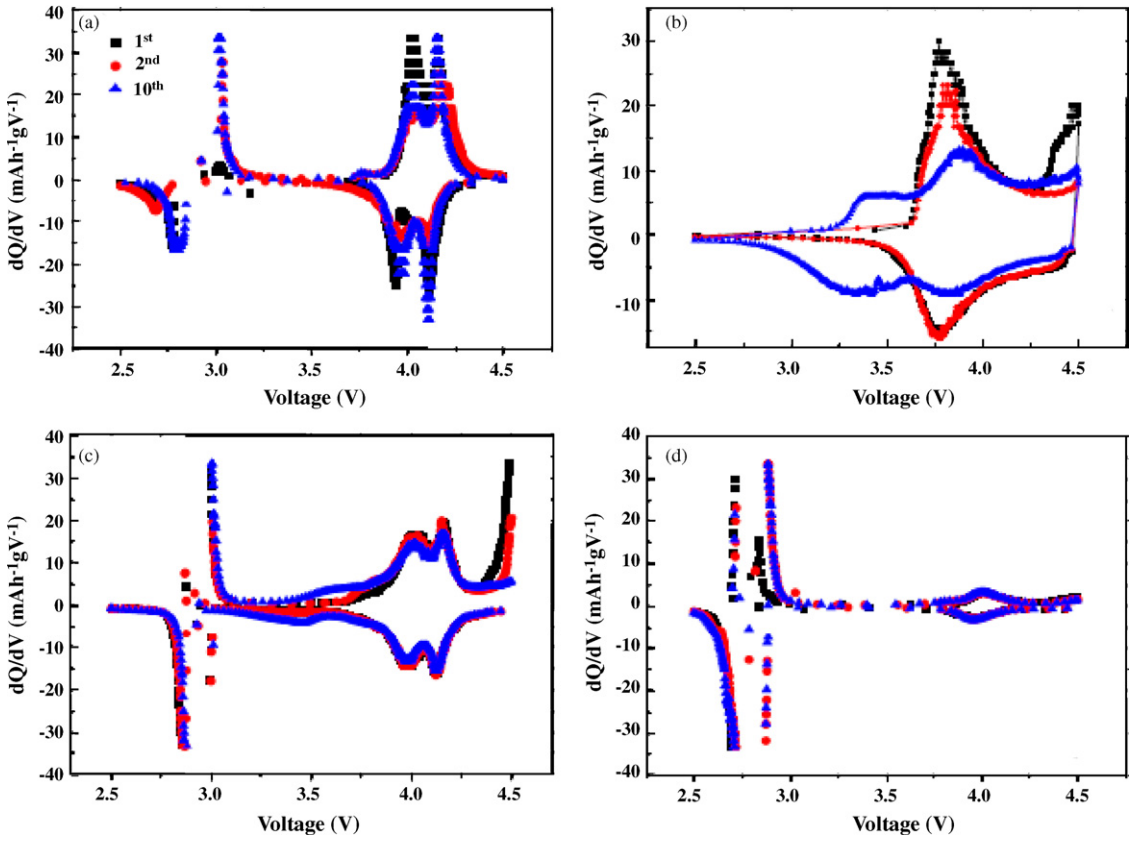

Fig. 2. Differential capacity vs. potential for (a) sample S1, (b) sample S2, (c) sample S3 and (d) sample S4. Cut-off voltage 2.4–4.5 V.

charging process peaks have been observed between 3.7 and 4.1 V and are attributed to the oxidation of Ni^{2+} to Ni^{4+} in the layered $Li[Li_{1/15}Ni_{1/5}Co_{2/5}Mn_{1/3}]O_2$. The oxidation peak of Mn^{3+} to Mn^{4+} rises and ends at 3.5 V, which is not observed at the first charge process. A drastic increase in the oxidation peak above 4.46 V is due to the irreversible capacity which corresponds to an irreversible plateau (to be discussed later) in the first cycle. The reduction peaks of Ni^{4+} to Ni^{2+} and Mn^{4+} to Mn^{3+} appear in the discharge process around 3.7 and 3.3 V, respectively. Interestingly, no oxidation peak is seen from Mn^{3+} to Mn^{4+} during the first charge which indicates that the as-prepared samples were synthesized in oxidation state of 4^+. It can be seen from Fig. 2(c) (sample S3) both composite cathodes have higher anodic and cathodic currents in the potential region of 2.7–3.0 V when compared to pure $LiMn_2O_4$. This implies that $Li[Li_{1/15}Ni_{1/5}Co_{2/5}Mn_{1/3}]O_2$ is also active in this voltage region. Also the irreversible plateau region is observed above 4.46 V which means that the compound $Li[Li_{1/15}Ni_{1/5}Co_{2/5}Mn_{1/3}]O_2$ is active at the end of charge and discharge potential. On contrary, the $Li[Li_{1/15}Ni_{1/5}Co_{2/5}Mn_{1/3}]O_2$ is not that much active for the sample S4 (Fig. 2(d)) which is reflected in the discharge capacity also [32] (Table 1).

Table 1
Classification of the samples

Sample	Type
S1	$LiMn_2O_4$ (spinel)
S2	$Li/Li[Li_{1/15}Ni_{1/5}Co_{2/5}Mn_{1/3}]O_2$ (layer)
S3	Simple mixing
S4	Ball milling followed by calcinations at 800 °C

3.3. Charge–discharge studies

Fig. 3(a–d) shows the charge–discharge curves for the samples S1, S2, S3 and S4, respectively. The shape of the curves of sample S3 and S4 differ from the samples S1 and S2. The curves show combine features of both samples S1 and S2. The fact that the discharge profile of the simple mechanical mixture (Fig. 3(c)) occurs in two steps suggest the independent discharge profiles of the constituent oxides. However, the single plateau observed in the case of the calcined mixture (Fig. 3(d)) suggests the formation of an inter-oxidic product. The corresponding discharge capacity vs. cycle number for the samples S1, S2, S3 and S4 are, respectively, depicted in Fig. 4(a–d). The samples S1, S2, S3 and S4 deliver an initial discharge capacity of 125, 163, 147 and 68 mAh g^{-1}, respectively. The discharge capacity of the sample S2 increases with the increase of cycle number (up to 10 cycles) and remains constant. A similar study has been observed by Kang et al. [32] where the authors reported the cycling behavior of $Li[Li_{0.2}Ni_{0.2}Mn_{0.6}]O_2$. According to the authors, the lithium ions are not completely removed during the first charge nor reinserted reversibly in the subsequent cycles. Li-ions in the transition metal layers are not removed completely during the initial cycling and this causes an increase in the discharge capacity. At the end of 50th cycles, sample S1 shows a discharge capacity of 90 mAh g^{-1} with a fade in capacity of 0.7 mAh g^{-1} per cycle. Although the sample S4 exhibits a lesser discharge capacity than that of S1, a stable cycling behavior was achieved. But the sample S2 exhibits higher discharge capacity than that of S1 and a stable cycling behavior was achieved. The enhanced cycling stability of $LiMn_2O_4$ has been attributed to the presence of $Li[Li_{1/15}Ni_{1/5}Co_{2/5}Mn_{1/3}]O_2$

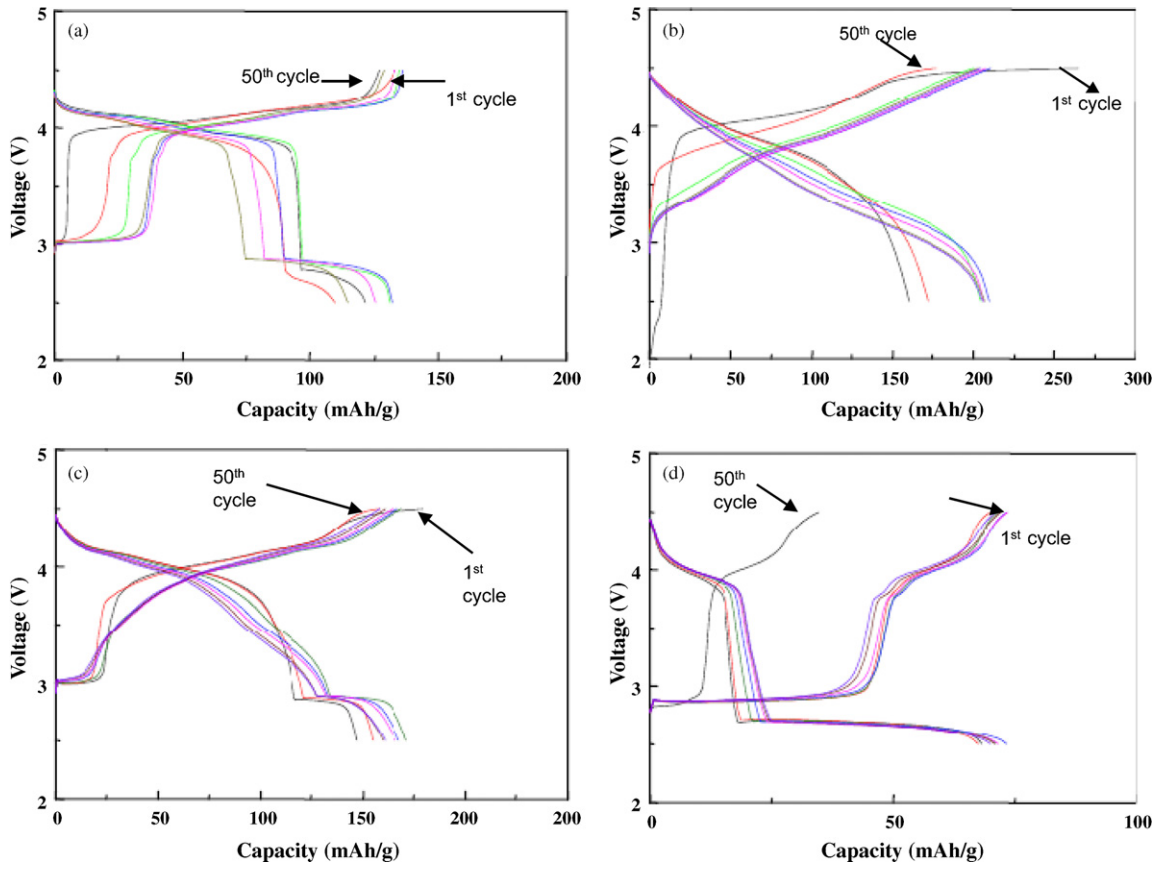

Fig. 3. Charge–discharge curves of the samples (a) S1, (b) S2, (c) S3 and (d) S4.

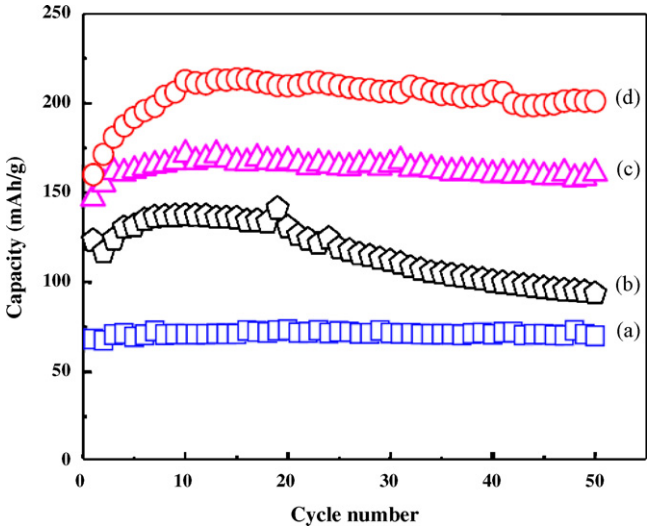

Fig. 4. Discharge capacity vs. cycle number for the cells (a) sample S1, (b) sample S2, (c) sample S3 and (d) sample S4.

in the $LiMn_2O_4$ which may prevent both over charge and over discharge of $LiMn_2O_4$ when operating above 4.1–4.2 V plateau [16].

4. Conclusion

The initial discharge capacity of $LiMn_2O_4$ material was considerably enhanced upon blending the material with $Li[Li_{1/15}Ni_{1/5}Co_{2/5}Mn_{1/3}]O_2$. The blend cathode material of $LiMn_2O_4$ and $Li[Li_{1/15}Ni_{1/5}Co_{2/5}Mn_{1/3}]O_2$ with a weight ratio of 1:1 by simple mixing exhibited higher discharge capacity and a stable cycling ability than the material calcined after ball milling. The poor cycling behavior of blend cathode material followed by calcination is attributed to the crystal defects which arise out of ballmilling.

Acknowledgement

This work was supported by the Korea Research Foundation Grant funded by the Korean Government (MOEHRD) (KRF-2005-005-J07501).

References

[1] M.M. Thackeray, Prog. Solid State Chem. 25 (1997) 1.
[2] C.H. Song, A.M. Stephan, S.K. Jeong, Y.J. Hwang, A.R. Kim, K.S. Nahm, J. Electrochem. Soc. 153 (2006) A390.
[3] P.G. Bruce, A.R. Armstrong, R.A. Gitzendanner, J. Mater. Chem. 9 (1999) 193.
[4] M.G.S.R. Thomas, P.G. Bruce, J.B. Goodenough, J. Electrochem. Soc. 132 (1985) 1521.
[5] K. Amine, H. Tukamoto, H. Yasuda, Y. Fujita, J. Electrochem. Soc. 143 (1996) 1607.
[6] Y. Xia, T. Sakai, T. Fujieda, M. Wada, H. Yoshinaga, Electrochem. Solid State Lett. 4 (2001) A49.
[7] K.A. Striebel, A. Rougier, C.R. Horne, R.P. Reade, E.J. Cairns, J. Electrochem. Soc. 146 (1999) 4339.
[8] G.T.K. Fey, C.Z. Lu, T. Prem Kumar, J. Power Sources 115 (2003) 332.
[9] A.M. Stephan, Dale-Teeters Electrochim. Acta 48 (2003) 2143.
[10] D.H. Jiang, Y.J. Shin, S.M. Oh, J. Electrochem. Soc. 143 (1996) 2204.
[11] A. Hirano, R. Kanno, Y. Kawamoto, Y. Takeda, M. Ohashi, Y. Yamaguchi, Solid State Ionics 78 (1995) 123.
[12] C. Delmas, I. Saadoune, A. Rougier, J. Power Sources 43/44 (1993) 595.
[13] G.T.K. Fey, R.F. Shiu, V. Subramanian, J.G. Chen, J. Power Sources 103 (2002) 265.
[14] T. Ohzuku, A. Ueda, T. Hirai, Chem. Express 7 (1992) 193.

[15] J.M. Kim, H.T. Chung, Electrochim. Acta 49 (2004) 937.
[16] Z.F. Ma, X.Q. Yang, X.Z. Lia, X. Sun, J. McBreen, Electrochem. Commun. 3 (2001) 425.
[17] T. Numata, C. Amemiya, T. Kumeuchi, M. Shirakata, M. Yonezawa, J. Power Sources 97/98 (2001) 358.
[18] S.T. Myung, M.H. Cho, H.T. Hong, T.H. Kang, C.S. Kim, J. Power Sources 146 (2005) 222.
[19] H. Huang, P.G. Bruce, J. Electrochem. Soc. 141 (1994) L106.
[20] K.M. Shaju, G.V. Subba Rao, B.V.R. Chowdari, Electrochim. Acta 48 (2002) 145.
[21] D.D. MacNeil, Z. Lu, J.R. Dahn, J. Electrochem. Soc. 149 (2002) A1132.
[22] Z. Lu, D.D. MacNeil, J.R. Dahn, Electrochem. Solid State Lett. 4 (2001) A200.
[23] T.H. Cho, S.M. Park, M. Yoshio, T. Hirai, Y. Hideshima, J. Power Sources 142 (2005) 306.
[24] P. Suresh, S. Rodrigues, A.K. Shukla, Solid State Ionics 176 (2005) 281.
[25] S.T. Myung, M.H. Lee, S. Komaba, N. Kumagai, Y.K. Sun, Electrochim. Acta 50 (2005) 4800.
[26] S.K. Jeong, C.H. Song, K.S. Nahm, A.M. Stephan, Electrochim. Acta 52 (2006) 885.
[27] J. Morales, C.P. Vincente, J.L. Tirado, Mater. Res. Bull. 39 (1990) 623.
[28] P. Suresh, A.K. Shukla, N. Munichadraiah, J. Power Sources 161 (2006) 1307.
[29] S. Wu, M. Yu, J. Power Sources 165 (2007) 660.
[30] Y. Xia, M. Yoshio, J. Electrochem. Soc. 143 (1996) 825.
[31] B.J. Hwang, R. Santhanam, D.G. Liu, J. Power Sources 97/98 (2001) 443.
[32] S.-H. Kang, Y.K. Sun, K. Amine, Electrochem. Solid State Lett. 6 (2003) A183.